4

The two-layer system

The next conceptual model of double-diffusive convection described in this monograph consists of a sharp interface sandwiched between two deep well-mixed layers. Such a configuration, illustrated in Figure 4.1, is particularly common in laboratory studies. Aside from considerations of simplicity and convenience, the two-layer model is motivated by observations of stepped structures in vertical temperature and salinity profiles known as thermohaline staircases – their origin and dynamics will be discussed in Chapter 8. The layered and gradient (Chapter 3) systems should not be regarded as mutually exclusive. For instance, flux-gradient finger models may be applicable locally for the interior region of double-diffusive interfaces. Furthermore, in nature it is often difficult to categorize a system as layered or gradient. Oceanographic observations frequently reveal irregular "steppiness" of T–S profiles (e.g., Schmitt and Evans, 1978), which apparently reflects elements of both layered and gradient dynamics. Nevertheless, the concept of a double-diffusive interface plays a prominent role in the development of double-diffusion theory for both salt-finger and diffusive regimes, warranting a detailed discussion. The central problem in the two-layer model, or for that matter in any double-diffusive system, involves prediction of the vertical transport of diffusing components. We start with the four-thirds interfacial flux law, originally proposed by Turner (1965, 1967) but approached here in a slightly different manner.

4.1 Interfacial flux laws

Consider a system consisting of two nearly homogeneous layers, separated by a high-gradient interface, as shown in Figure 4.1 for the salt-finger (a) and diffusive (b) cases. In both models, homogeneous stratification in the layers is maintained by top-heavy convection, which, in turn, is driven by the unequal transport of heat and salt through the double-diffusive interface. For the salt-finger case (Fig. 4.1a) fluxes of heat and salt are downward (i.e., negative). The contribution of salt flux to

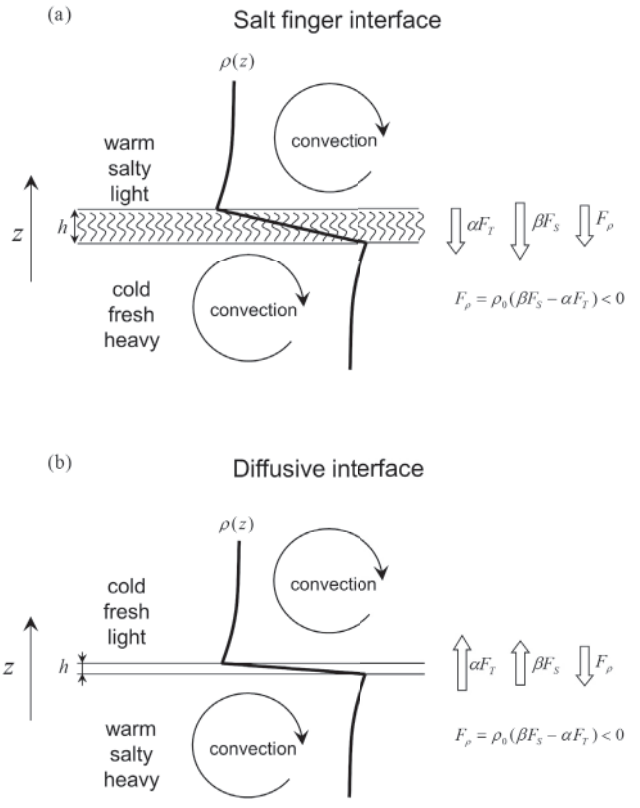

Figure 4.1 Schematic diagrams illustrating the dynamics of two-layer fingering (a) and diffusive (b) systems.

density flux exceeds that of heat, as measured by the flux ratio $\gamma < 1$ (Chapter 2) and therefore the transport of salt controls the direction of the net density flux – it is also downward. Thus, fluid at the top of the lower layer, immediately below the interface, consistently gains density and maintains convection. Fluid immediately above the interface loses density, which drives convection in the upper layer.

The physics of the diffusive system (Fig. 4.1b) is somewhat different. Transport of heat and salt is controlled by molecular diffusion across the interface, particularly for moderate density ratios. Therefore, the direction of density transport is controlled by heat (faster diffuser). As heat diffuses from the warm lower layer into the cold upper layer, fluid immediately above (below) the interface becomes lighter (denser), forcing convection in both layers. Ultimately, the motion in diffusive and salt-finger systems is driven by the release of potential energy stored in the unstably stratified components. As the upper layer becomes lighter and the lower

layer denser, the center of mass is displaced downward and the released potential energy is partially converted into kinetic energy.

In both configurations, salt-finger and diffusive, it is natural to assume that the behavior and transport characteristics of a two-layer system are determined by the differences in temperature and salinity between the mixed layers. Furthermore, it is not just the variation in T and S but rather their contribution to buoyancy that controls the dynamics. To make this point more evident, the governing equations (1.1) and (1.2) are rewritten as follows:

$$\begin{cases} \dfrac{d\vec{\mathrm{v}}}{dt} = -\frac{\nabla p}{\rho_0} + (b_T + b_S)\vec{k} + \nu\nabla^2\vec{\mathrm{v}}, \\ \nabla \cdot \vec{\mathrm{v}} = 0, \\ \dfrac{db_T}{dt} = k_T\nabla^2 b_T, \\ \dfrac{db_S}{dt} = k_S\nabla^2 b_S, \end{cases} \tag{4.1}$$

where $b_T = g\alpha(T - T_0)$ and $b_S = g\beta(S - S_0)$ are the buoyancy components due to temperature and salinity. In (4.1) and throughout this chapter, we use dimensional quantities.

Of particular interest are the vertical fluxes of buoyancy components $\left(F_{b_T}, F_{b_S}\right)$ across the double-diffusive interface and its thickness (h). These quantities are assumed to be determined by the variation of buoyancy components across the interface ($\Delta b_T, \Delta b_S$) and by molecular characteristics (k_T, k_S, ν):

$$\begin{cases} F_{b_T} = F_{b_T}(\Delta b_T, \Delta b_S, k_T, k_S, \nu), \\ F_{b_S} = F_{b_S}(\Delta b_T, \Delta b_S, k_T, k_S, \nu), \\ h = h(\Delta b_T, \Delta b_S, k_T, k_S, \nu). \end{cases} \tag{4.2}$$

Formulation (4.2) explicitly ignores the possible influence of the mixed layer thickness. Layers are assumed to be sufficiently deep so that the bottom and surface of the working fluid are too separated from the interface to affect processes operating in its immediate vicinity. Also neglected are evolutionary effects, such as the role of the initial thickness of the interface. While these assumptions have to be critically reexamined on a case-by-case basis, it will be shown shortly that the interfacial flux model based on (4.2) is reasonably successful in explaining some observations and laboratory experiments.

The next step involves the dimensional argument, elegantly expressed by the Buckingham (1914) π-theorem: each non-dimensional combination is controlled by other non-dimensional combinations or π-groups. Principles of dimensional analysis and examples of its application have been discussed in numerous fluid dynamical texts (e.g., Barenblatt, 1996; Kundu and Cohen, 2008). In our case,

the expression for the quantity of interest – F_{b_T} in (4.2) – involves six independent variables in two fundamental units, time (s) and length (m) : $F_{b_T}[\mathrm{m^2\ s^{-3}}]$; Δb_T, $\Delta b_T[\mathrm{m\,s^{-2}}]$; and $k_T, k_S, \nu[\mathrm{m^2\,s^{-1}}]$. Thus, we can expect a functional relation between four independent π-groups. The non-dimensional combination involving F_{b_T}, Δb_T and k_T is easily constructed:

$$\pi_1 = \frac{F_{b_T}}{(\Delta b_T)^{\frac{4}{3}} k_T^{\frac{1}{3}}}. \tag{4.3}$$

Other non-dimensional combinations of variables in (4.2) are familiar from previous chapters; they are the density ratio $R_\rho = \frac{\Delta b_T}{\Delta b_S}$, the diffusivity ratio $\tau = \frac{k_S}{k_T}$ and the Prandtl number $Pr = \frac{\nu}{k_T}$. Applying Buckingham's theorem to these π-groups yields:

$$\frac{F_{b_T}}{(\Delta b_T)^{\frac{4}{3}} k_T^{\frac{1}{3}}} = C_T(R_\rho, \tau, Pr). \tag{4.4}$$

Function C_T cannot be determined internally by the dimensional theory and requires experimental or numerical calibration. Expressing (4.4) in terms of temperature rather than buoyancy reduces it to

$$\alpha F_T = (k_T g)^{\frac{1}{3}} C_T (\alpha \Delta T)^{\frac{4}{3}}. \tag{4.5}$$

The same reasoning can be applied to the salt flux:

$$\beta F_S = (k_T g)^{\frac{1}{3}} C_S (\beta \Delta S)^{\frac{4}{3}}, \tag{4.6}$$

where C_S is a yet unknown function of $\left(R_\rho, Pr, \tau\right)$. Expressions (4.5) and (4.6) are referred to as the "four-thirds flux laws" for double-diffusive convection (Turner, 1965, 1967, 1979). As in the gradient model (Chapter 3), the vertical transfer properties of the two-layer system are often characterized by the flux ratio:

$$\gamma(R_\rho, \tau, Pr) = \frac{\alpha F_T}{\beta F_S} = \frac{C_T}{C_S} R_\rho^{\frac{4}{3}}. \tag{4.7}$$

When the dimensional argument is applied to the interfacial thickness (h), we arrive at

$$h = \left(\frac{k_T^2}{g}\right)^{\frac{1}{3}} C_h(R_\rho, \tau, Pr)(\alpha \Delta T)^{-\frac{1}{3}}. \tag{4.8}$$

To put these results into historical perspective, it should be mentioned that Turner originally arrived at the four-thirds laws as a plausible extension of a classical model for turbulent thermal convection (Priestley, 1954; Howard, 1963). This model assumes a unique power law relation between the Nusselt number $Nu = \frac{F_T}{k_T \Delta T/H}$, a non-dimensional measure of heat transport, and the Rayleigh

number $R = \frac{g\alpha\Delta T H^3}{k_T \nu}$, measuring the strength of thermal forcing:

$$Nu \propto R^n. \tag{4.9}$$

The assumption that the heat flux is independent of the depth of the convective zone (H) specifies the exponent $n = \frac{1}{3}$. This prescription for the Nusselt number is equivalent to the four-thirds flux law $F_T \propto \Delta T^{\frac{4}{3}}$, the counterpart of (4.5). While it seems sensible to assume that the turbulent fluxes are not affected by H as long as it is sufficiently large, subsequent studies of single-component convection have revealed systematic deviations from the four-thirds flux law (e.g., Grossmann and Lohse, 2000). In both problems – thermal and double-diffusive convection – the assumed lack of importance of layer depths, initial conditions and evolutionary history can be questioned. Nevertheless, the four-thirds flux law provides a convenient starting point for the discussion of experiments and observations. It has some success in explaining the salient features of layered double-diffusive systems. Caution is advised though for sensitive problems that require precise models of the interfacial fluxes.

4.2 Salt-finger interfaces

A major source of information on the dynamics of interfaces, both fingering and diffusive, has traditionally been provided by laboratory experiments. The first quantitative experiment with salt-finger interfaces was performed by Turner (1967). Figure 4.2 shows a schematic of the experimental setup (right panel) and salt fingers forming on the interfaces (left panel) – this particular experiment contained three mixed layers separated by two interfaces. Turner's work for the first time offered an estimate of the heat–salt flux ratio, which was shown to be nearly uniform with $\gamma \approx 0.56$ over the wide range $2 < R_\rho < 10$. This result was, to large extent, confirmed and reproduced by subsequent laboratory and numerical studies. Technical complications prevented Turner from measuring the flux ratio for lower values of R_ρ, although he speculated that γ should increase with decreasing density ratio, approaching unity at $R_\rho = 1$. More accurate measurements were taken by Schmitt (1979b), whose experiments (i) supported the four-thirds flux law to within the experimental uncertainties, (ii) yielded Stern numbers (3.5) of order one, and (iii) revealed the gentle variation in the flux ratio with R_ρ. Schmitt's experiments were followed by McDougall and Taylor (1984). Changes to the experimental procedure in the latter study made it possible to examine a lower range of density ratios and smaller T–S contrasts between the upper and lower layers – a welcome adjustment towards typical oceanic conditions. The results in McDougall and Taylor (1984) were broadly consistent with Schmitt (1979b), although some quantitative

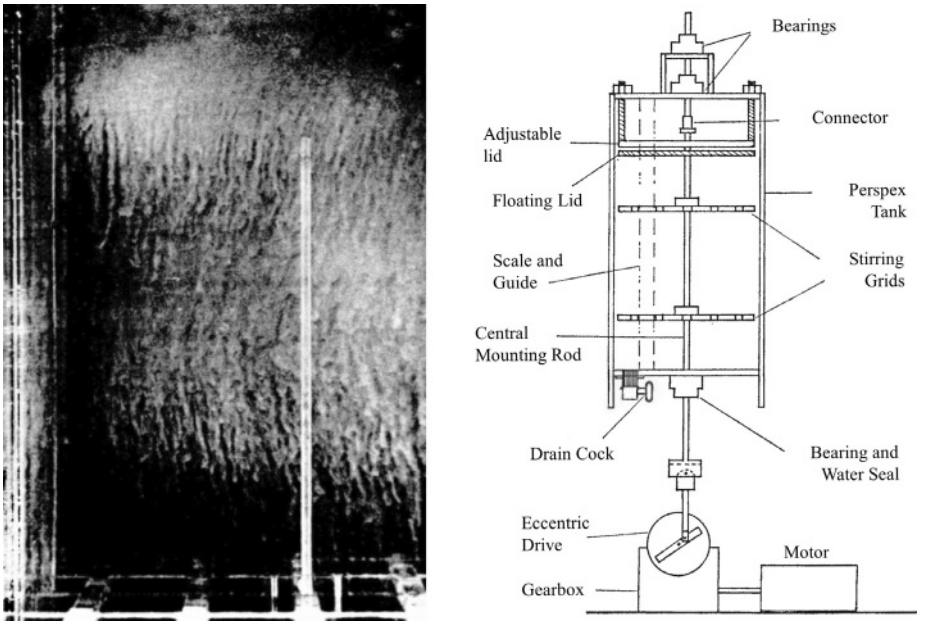

Figure 4.2 Formation of salt fingers across two high-gradient interfaces (left). Schematic of the experimental apparatus is shown in the right panel. From Turner (1967).

differences emerged. The values of Stern number and flux ratios were consistently higher in McDougall and Taylor and the 4/3 exponent in (4.6) was revised downward to 1.23.

The experiments of Taylor and Bucens (1989) revealed in greater detail the spatial and temporal patterns of salt fingers – see the shadowgraphs in Figure 4.3. Salt fingers in a two-layer system are irregular, time dependent and vertically coherent over only a fraction of the interfacial region. Overall, the structure of interfacial fingers is similar to that in extended gradient layers (cf. Fig. 3.14). Interestingly, Taylor and Bucens' study reported systematic quantitative differences in transport characteristics relative to earlier investigations. The disagreement was attributed to the differences in the experimental setup, such as the quiescent initial state in McDougall and Taylor's experiments and the presence of mechanical perturbations in Turner (1967) and Schmitt (1979b). The sensitivity to such details has significant implications for the dynamics of layered double-diffusive systems. The derivation of the four-thirds flux law necessarily assumes a unique solution for fluxes. The variation of *T–S* transport in response to very modest changes in configuration suggests that fluxes are not entirely determined by the temperature and salinity contrasts, giving a legitimate reason to question (4.2) and thus the flux laws themselves. This concern becomes particularly worrisome when the

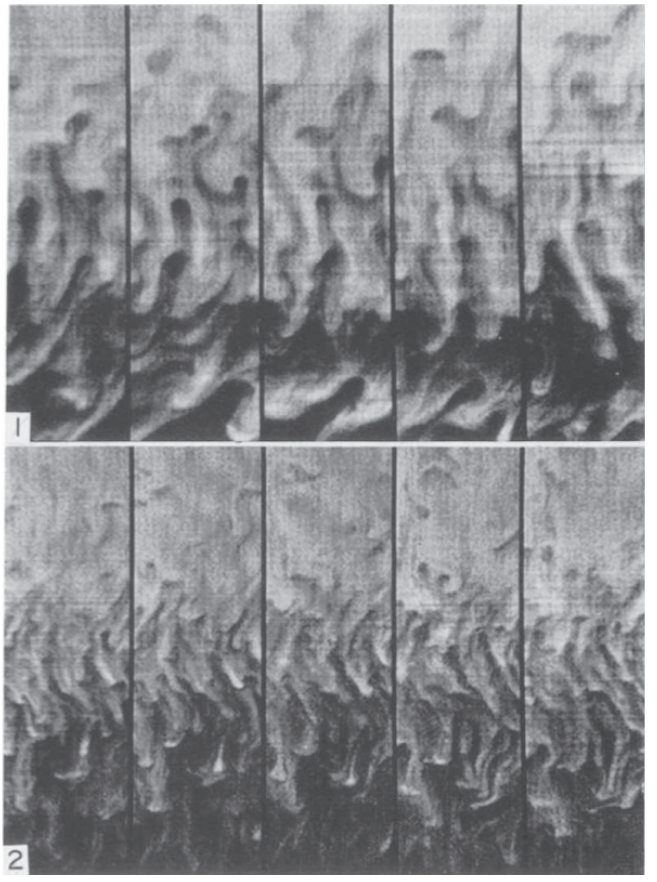

Figure 4.3 Each panel shows successive images of a part of the finger interface in the two-layer laboratory experiment. The upper panel shows the state recorded for $R_\rho = 2.46$ and the lower panel shows the later stage of the same experiment when R_ρ had increased to 2.75. The images in each panel were captured 5 seconds apart. From Taylor and Bucens (1989).

four-thirds law is applied to oceanic staircases. Clearly, the oceanographic situation contains many ingredients that are absent in the laboratory analogue – internal waves, an energetic eddy field and large-scale shear, to name just a few. Therefore, it is not surprising that extrapolation of the laboratory-calibrated four-thirds flux law to the staircase in the Western Atlantic overestimated the vertical transport by an order of magnitude (Kunze, 1987). While this mismatch has never been fully explained, the lack of uniqueness in the formulation of the flux laws is likely to play a role.

An important role in the analysis of the double-diffusive two-layer system is played by laboratory experiments in which heat and salt are replaced by two solutes with different molecular diffusivities. Such experiments were initially proposed to

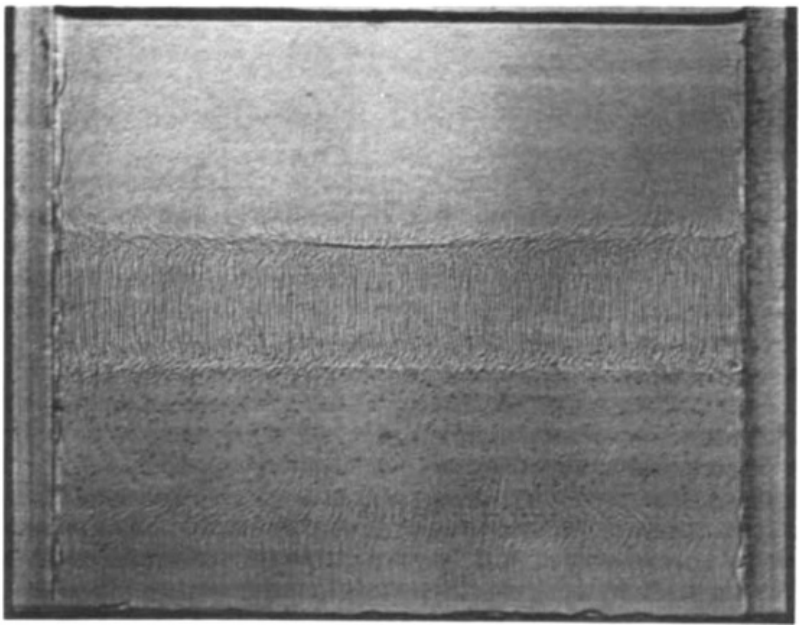

Figure 4.4 Shadowgraph of a finger interface formed by placing a layer of sucrose solution on top of a denser salt solution. From Turner (1985).

avoid spurious effects due to sidewall cooling and heating. This approach was pioneered by Stern and Turner (1969), who chose sugar and salt as two diffusing components for both two-layer and uniform-gradient (Chapter 3) experiments. This study was followed by progressively more precise measurements by Lambert and Demenkow (1972), Griffiths and Ruddick (1980) and Taylor and Veronis (1996).

The insights brought by the two-layer salt–sugar experiments are difficult to overestimate. The exploration of a completely different, relative to the heat–salt experiments, parameter regime made it possible to identify generic characteristics of double-diffusive convection and fluid-dependent features. The sugar–salt fingers (Fig. 4.4) are typically more regular and vertically elongated than the heat–salt fingers (compare with Figs. 4.2 and 4.3). The more organized and steady flow character of the salt–sugar system permitted visualization of the horizontal cell structure of the interfaces. Shirtcliffe and Turner (1970) used a simple and ingenious optical system (Fig. 4.5a) and discovered that the interfacial fingers have a remarkably regular square cross-section (Fig. 4.5b). In view of the degeneracy of the linear theory with respect to the planform selection (Chapter 2), the preference for the square cells must be due to the nonlinear interactions between various finger modes.

There are numerous quantitative differences in the transport characteristics of heat–salt and salt–sugar systems. For instance, Stern numbers (A) in salt–sugar

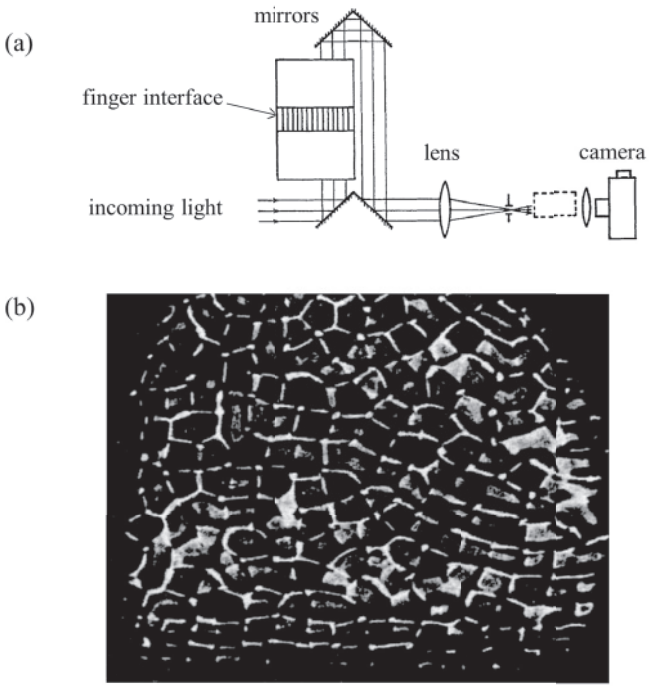

Figure 4.5 (a) The optical system designed to observe the cell structure of fingers in the laboratory experiment. This system was used to capture the image (b) of the horizontal pattern at the mid-plane of the fingering interface. From Shirtcliffe and Turner (1970).

experiments are much lower than in their heat–salt counterparts. Lambert and Demenkow (1972) report values as low as $A = 2 \cdot 10^{-3}$, casting doubt on the generality of Stern's number criterion for the magnitude of salt fingers (a controversial issue discussed in Section 3.2). The coefficient $C'_S = C_S(k_T g)^{\frac{1}{3}} = \frac{\beta F_S}{(\beta \Delta S)^{\frac{4}{3}}}$ of the flux law (4.6) recorded in the salt–sugar experiments (e.g., Griffiths and Ruddick, 1980; Taylor and Veronis, 1996) also differs from the heat–salt values. It rapidly decreases from $C'_S \sim 10^{-4}\,\mathrm{m\,s^{-1}}$ at R_ρ close to unity to $C'_S \sim 10^{-6}\,\mathrm{m\,s^{-1}}$ for $R_\rho \sim 2$. In the heat–salt experiments, the flux law coefficients are typically on the order of $C'_S \sim 10^{-3}\,\mathrm{m\,s^{-1}}$ and exhibit much more limited variation with the density ratio (Schmitt 1979b; McDougall and Taylor, 1984; Taylor and Bucens, 1989).

Of course, sensitivity of C'_S to the molecular characteristics of diffusing substances is perfectly natural and fully consistent with the flux law formulation. However, salt–sugar experiments have also underscored more fundamental uncertainties with regard to the four-thirds law. Taylor and Veronis (1996) compared their estimates of the flux law coefficient with earlier measurements in Griffiths and Ruddick (1980) and documented the systematic offset between the two. This

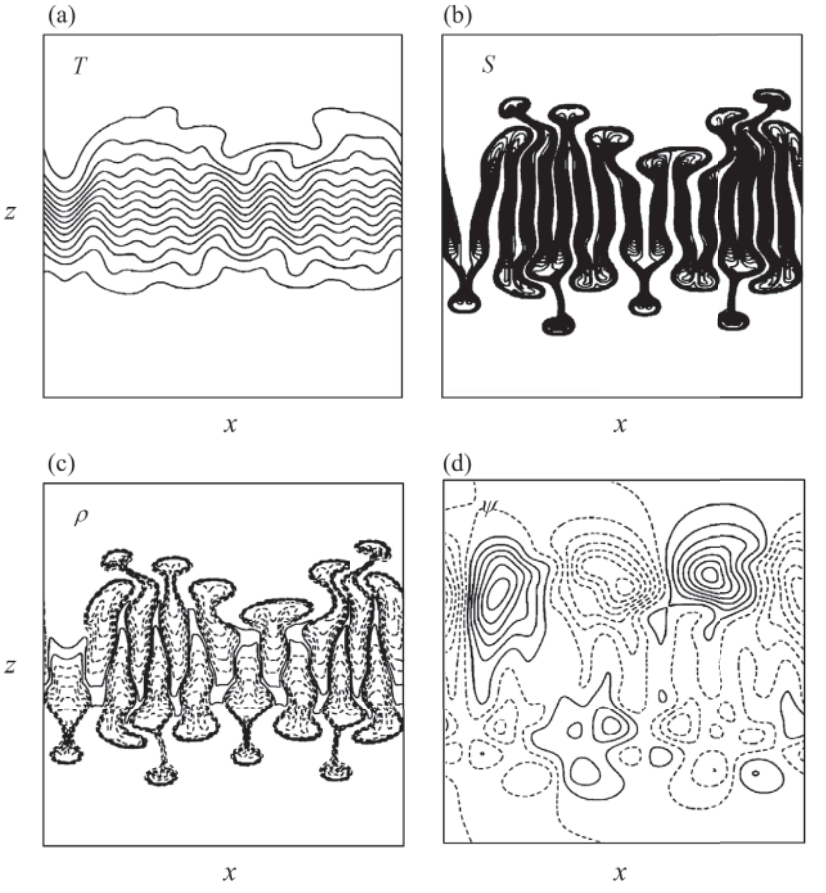

Figure 4.6 Two-dimensional numerical simulation of salt fingering. Contour plots of (a) T, (b) S, (c) ρ and (d) ψ are shown for a system of eight fingers forming across the interface separating two homogeneous layers. From Shen and Veronis (1997).

offset can be interpreted as a manifestation of a non-unique relation between vertical fluxes and the variation of properties between the layers. Echoing a similar concern of Taylor and Bucens (1989) for heat–salt interfaces, Taylor and Veronis (1996) suggested that the four-thirds law should not be applied indiscriminately to fingering convection.

Numerical simulations of the two-layer configuration (Shen, 1993; Shen and Veronis, 1997; Ozgokmen *et al*., 1998; Paparella, 2000) have been generally successful in reproducing major features of laboratory experiments. The patterns of fingers forming in the interfacial zone – see Shen and Veronis (1997) simulations in Figure 4.6 – resemble their laboratory analogues. Numerical models consistently reproduced typical values of vertical fluxes, the flux ratio, Stern number,

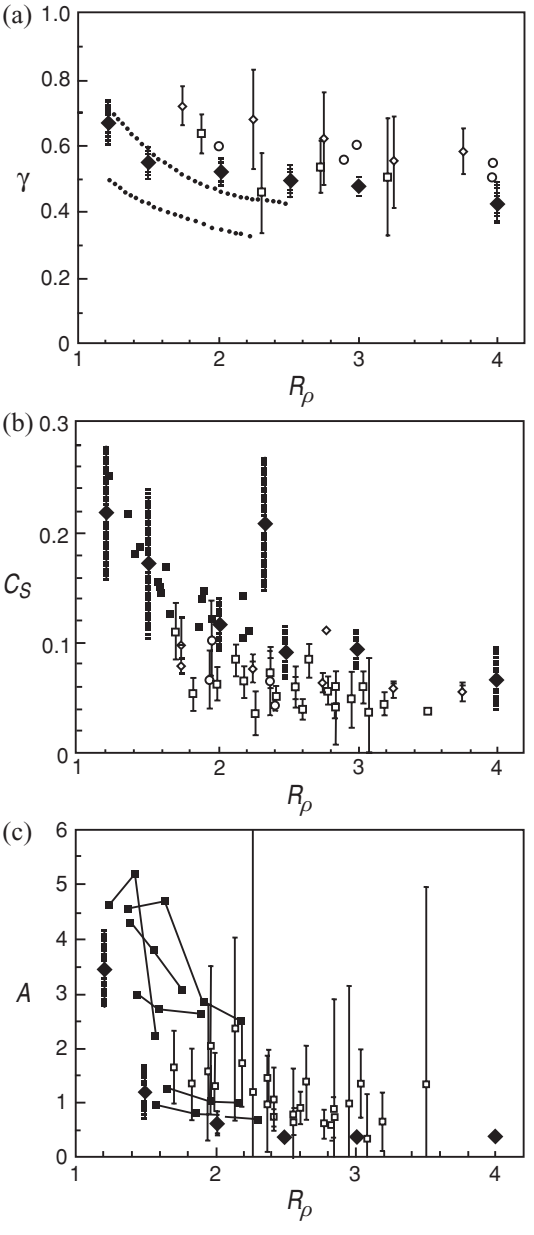

Figure 4.7 Comparison of numerical and laboratory estimates of (a) the flux ratio γ, (b) coefficient of the four-thirds flux law C_S and (c) the Stern number A. Values from the numerical experiments are marked with ♦. The laboratory data are given by ◊ (Schmitt, 1979b), □ (Taylor and Bucens, 1989), ○ (Turner, 1967), ■ (McDougall and Taylor, 1984) and the dotted curves in (a) mark the range of McDougall and Taylor's measurements. From Shen (1993).

Table 4.1 *A summary of two-layer flux laws in the form* $F_S \propto (\Delta S)^p$ *for salt-finger (SF) and diffusive convection (DC)*

Model	Form of double-diffusion	Flux law exponent (p)	Basis
Schmitt (1979b)	SF	1.24–1.37	Expts.
McDougall and Taylor (1984)	SF	1.23	Expts.
Krishnamurti (2003)	SF	1.18–1.19	Expts.
Ozgokmen *et al*. (1998)	SF	4/3	DNS
Paparella (2000)	SF	1.33–2.0	DNS
Sreenivas *et al*. (2009)	SF	1.32	DNS
Marmorino and Caldwell (1976)	DC	1.32–1.34	Expts.
Kelley *et al*. (2003)	DC	1.27–1.47	Expts.

The exponent p is obtained by fitting the experimental (Expts.) or numerical (DNS) data.

and the pattern of their variation with R_ρ (Fig. 4.7). Unfortunately, simulations have so far not provided a definitive answer regarding the utility of the four-thirds flux law. Sreenivas *et al*. (2009) found their simulations to be well described by (4.6). Ozgokmen *et al*. (1998) reported the overall adequate performance of the four-thirds law, noting certain inconsistencies during the initial phase of system adjustment to the quasi-equilibrium state and the final run-down phase followed by the disintegration of layered structure. Paparella (2000), on the other hand, suggested that the exponent of the flux law consistently exceeds 4/3. Several studies, summarized in Table 4.1, proposed empirical adjustments to the four-thirds law in the form

$$F_S \propto (\Delta S)^p \,. \tag{4.10}$$

The exponent p was estimated by fitting (4.10) to experimental or numerical data. In most cases, the modifications of the four-thirds flux law fall within the statistical error bars. However, at this point we reiterate that the adequate performance of the four-thirds law in a single simulation – or even in a set of similarly designed simulations – does not fully validate it. If the flux law coefficient C_S depends on the setup of an experiment, numerical or laboratory, then the practical use of the four-thirds law may be limited.

4.3 Diffusive interfaces

Despite significant differences in the dynamics of diffusive and salt-finger interfaces, similarities in the historical development of the two problems are apparent.

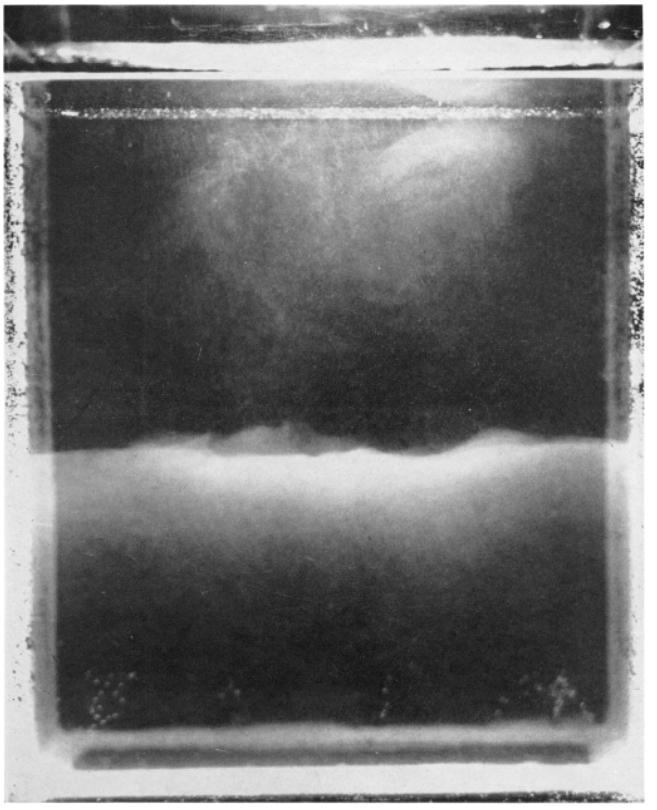

Figure 4.8 Laboratory experimentation with the two-layer diffusive system. The lower, more saline layer has been colored with fluorescent dye. From Turner (1965).

The first insights into the diffusive case were also brought by laboratory experiments. Figure 4.8 presents Turner's (1965) experiment in which the two-layer system, initially stratified only with respect to salinity, was heated from below. The heating rate was sufficiently weak and the lower layer remained denser than the upper one throughout the duration of the experiment. Turner's study quantified the dependencies of temperature and salinity fluxes on the diffusive density ratio (R_ρ^*). Both heat and salt fluxes monotonically increased with decreasing R_ρ^* – an expected consequence of decreasing density stratification. Figure 4.9a presents the heat flux across the interface normalized by the "solid plane value" – the flux realized in pure thermal convection bounded by rigid horizontal planes with the same temperature variation. The solid plane flux was evaluated using the experimentally calibrated four-thirds flux law (Chandrasekhar, 1961). For relatively high density ratios ($R_\rho^* > 2$), the actual heat flux is less than the corresponding solid plane value, which reflects the tendency of salinity stratification to suppress the vertical motion

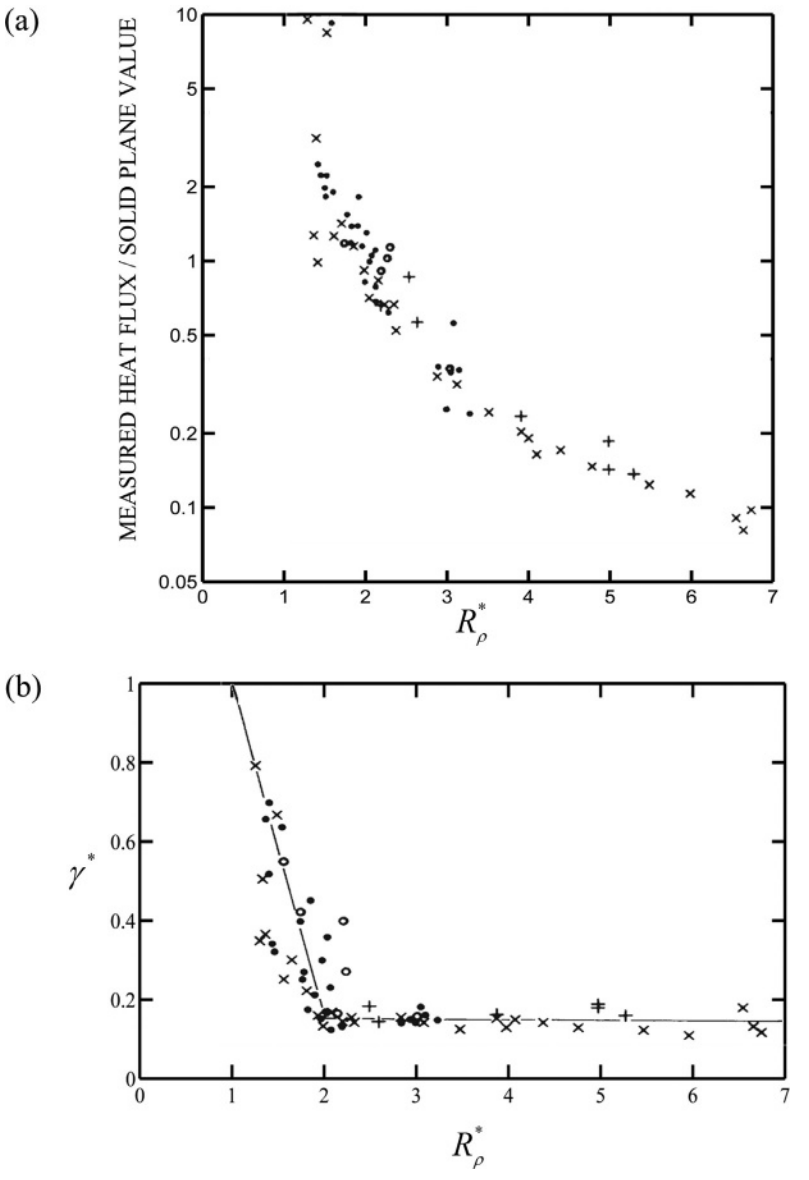

Figure 4.9 (a) The measured heat flux across the diffusive interface in Figure 4.8, normalized by the solid plane value and plotted against the diffusive density ratio. (b) The flux ratio as a function of the density ratio. From Turner (1965).

of fluid and thus heat transfer. However, the opposite is true for $R_\rho^* < 2$: the heat flux exceeds the solid plane value by as much as an order of magnitude. Such a dramatic effect is attributed to the eddy transfer across the interface, which for low R_ρ^* becomes strongly time dependent. The latter effect was examined in greater

detail by Stamp *et al*. (1998). The pattern of the flux ratio in Figure 4.9b is even more intriguing. The sharp decrease in $\gamma^* = \frac{\beta F_S}{\alpha F_T}$ with R_ρ^* for relatively low density ratios (variable regime) is followed by the uniform flux ratio of $\gamma^* \approx 0.15$ for $R_\rho^* > 2$ (constant regime).

Undoubtedly inspired by the salt-finger experiments of Stern and Turner (1969), several experimentalists used isothermal aqueous salt and sugar solute to investigate the dynamics of diffusive interfaces. Salt–sugar and heat–salt experiments reveal qualitatively similar patterns and behavior (see Fig. 1.6). The first diffusive two-layer salt–sugar experiment was performed by Shirtcliffe (1973). As in the heat–salt case (Turner, 1965) T-flux exceeds the solid plane value for low density ratios and falls below for high. However, in contrast to the heat–salt case, the flux ratio is nearly uniform for all experimental density ratios, not only the higher range. Shirtcliffe noticed that the flux ratio in the constant regime for both heat–salt and sugar–salt experiments can be approximated by

$$\gamma^* \approx \sqrt{\tau}. \tag{4.11}$$

This empirical conjecture was later rationalized by explicit mechanistic models of the diffusive interface (Linden and Shirtcliffe, 1978; Worster, 2004), although it should be mentioned that some laboratory experiments (Takao and Narusawa, 1980; Turner *et al*., 1970; Newell, 1984) find systematic departures from (4.11). Stern (1982) concluded, based on the application of variational methods to the diffusive two-layer system, that (4.11) represents the lower bound of the flux ratio.

Diffusive experiments have been reproduced, extended and improved numerous times in both heat–salt (Crapper, 1975; Marmorino and Caldwell, 1976; Newell, 1984; Taylor, 1988; among others) and salt–sugar (Turner and Chen, 1974; Turner, 1985; Stamp *et al*., 1998) systems. Most experimental results are qualitatively consistent with each other but differ on the quantitative level. An important distinction should be made between (i) run-down experiments, in which T and S are allowed to diffuse in time (e.g., Takao and Narusawa, 1980), (ii) run-up experiments (e.g., Turner, 1965) in which the system is heated from below, and (iii) quasi-equilibrium experiments (Marmorino and Caldwell, 1976) maintained in a steady state by a combination of heating from below and cooling from above. It should be kept in mind that only the last configuration can be truly steady. For the run-up and run-down experiments, an assumption is often made that the system passes through a series of quasi-equilibrium states, and therefore all theoretical steady-state arguments can be applied directly. This assumption is justified for low and intermediate values of density ratio and deep mixed layers, in which case the rate of evolution of the diffusive interface greatly exceeds that of the mixed layers. As density ratio increases, the quasi-steady model becomes progressively more questionable. An interesting time-dependent effect involves the systematic drift of the interface.

The interfacial drift becomes particularly strong at low density ratios and can be attributed either to the imbalance in the turbulent intensities in the adjoining layers (Marmorino and Caldwell, 1976) or to the nonlinearity of the equation of state (McDougall, 1981).

A comprehensive theoretical model of the diffusive interface was developed by Linden and Shirtcliffe (1978) and considerably extended by Worster (2004). The key features of these models are illustrated in Figure 4.10. The diffusive interface is represented by a laminar statically stable core region bounded from above and below by thin unstable boundary layers. Following ideas proposed for thermal convection from a heated plate (Howard, 1964), it is assumed that the boundary layers undergo cyclic growth and convective eruption, which maintains the boundary layers close to the marginally unstable state characterized by the critical Rayleigh number. To close the problem, the temperature and salinity jumps across the boundary layers in the model are also assumed to be compensating in terms of density – that is, density is supposed to vary continuously between the core of the diffusive interface and the mixed layers as shown in Figure 4.10a. Combining these assumptions leads to an explicit expression for the flux ratio (4.11), which elegantly explains the laboratory result. Linden and Shirtcliffe (1978) formulated the steady-state version of the model, deriving an expression for the equilibrium temperature flux:

$$F_T = \frac{1}{\pi^{\frac{1}{3}}} \frac{\left(1 - \tau^{\frac{1}{2}} R_\rho^*\right)^{\frac{4}{3}}}{\left(1 - \tau^{\frac{1}{2}}\right)^{\frac{1}{3}}} F_T^{SP}, \tag{4.12}$$

where F_T^{SP} is the solid plane value. From (4.12) it is apparent that no steady solution exists for $R_\rho^* > \tau^{-\frac{1}{2}}$. The mixed layer convection in this regime is no longer capable of arresting the diffusive spreading of the interface, which monotonically thickens in time (Newell, 1984).

Prediction (4.12) is qualitatively consistent with the laboratory results for the intermediate range of density ratios ($3 < R_\rho^* < 7$ for heat–salt and $1.2 < R_\rho^* < 1.65$ for salt–sugar experiments) but largely fails for lower and higher values of R_ρ^*. Both problems can be traced to the model assumptions. For low R_ρ^* the interface becomes turbulent and therefore the inability of the model to account for the eddy transport of heat and salt across the core leads to an underestimate of fluxes. Failure of the model for large density ratios can also be ascribed to time-dependent effects, albeit of a different kind. At high density ratios the adjustment of fluxes to changing background state is extremely slow and therefore the diffusive system no longer evolves through a series of quasi-steady states. In this regime, each current state depends sensitively on the past history of the system, which renders the steady-state model (4.12) largely inapplicable. The generalization of the Linden and Shirtcliffe

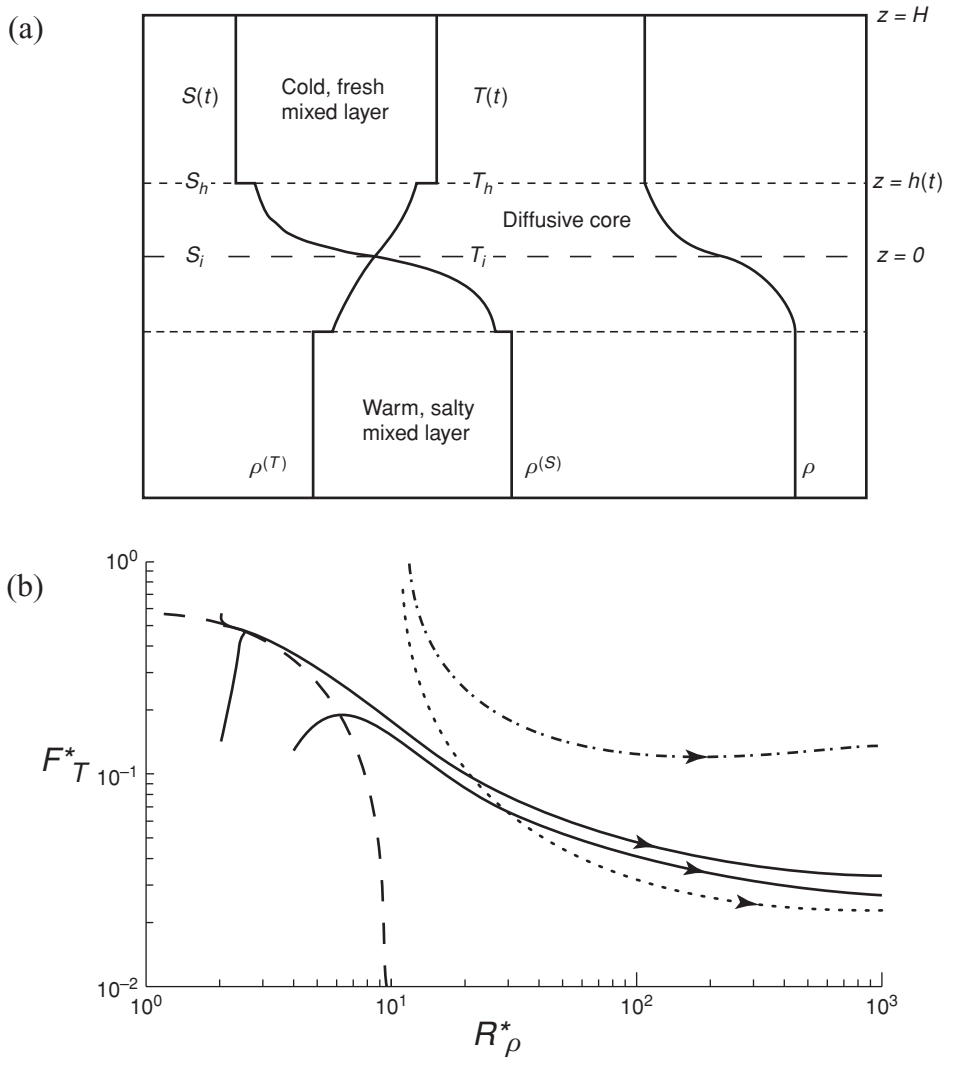

Figure 4.10 (a) Schematic diagram of a theoretical model for the two-layer diffusive system. (b) The evolutionary paths (curves with arrows) in the (R_ρ^*, F_T^*) plane predicted by the model in (a) for various initial conditions. F_T^* denotes the temperature flux normalized by the solid plane value. The long-dashed curve corresponds to the steady-state model of Linden and Shirtcliffe (1978). From Worster (2004).

(1978) model by Worster (2004), which takes these time-dependent dynamics into account, explains many features of laboratory experiments. It rationalizes the tendency of the diffusive system to approach the quasi-equilibrium state for intermediate density ratios and explains its evolutionary pattern for high R_ρ^*. The

time-dependent model also draws attention to the significance of initial conditions by demonstrating their long-term influence on the system (see Fig. 4.10b). In the parameter regime where steady-state balances are expected, the Linden–Shirtcliffe–Worster model is consistent with the four-thirds flux laws (4.5), (4.6) and the interfacial thickness law (4.8).

It should be noted that an alternative model of the two-layer diffusive system exists (Fernando, 1989) in which the interface is represented by a double boundary layer structure: the outer layer is controlled by the diffusion of heat and contains a much thinner salinity layer. Fernando (1989, 1990) finds some support for the double boundary layer model in the laboratory and field measurements. However, a more systematic analysis is needed to identify the relative merits of the single- and double-layer models of diffusive interfaces.